Available online at www.sciencedirect.com
SCIENCE DIRECT®
Thermochimica Acta 421 (2004) 211–215
thermochimica acta
www.elsevier.com/locate/tca

Thermal characterization during dehydration of nitrifying and denitrifying microbiological mud encapsulated in silica gel

G. Aguirre [a], G. Arriola [a], J. Gómez-Hernández [a], T. López [a], M. Picquart [a,*], D.H. Aguilar [b], P. Quintana [b], J.J. Alvarado-Gil [b]

[a] *Universidad Autónoma Metropolitana-Iztapalapa, A.P. 55-534, Mexico 09340, D.F., Mexico*
[b] *Cinvestav-IPN, Unidad Mérida, Departamento de Física Aplicada, A.P. 73. Cordemex, Mérida, Yucatán, Mexico 97310, Mexico*

Received 3 December 2003; received in revised form 12 February 2004; accepted 5 April 2004
Available online 21 July 2004

Abstract

An alternative method to diminish the nitrogen pollutant levels in waste waters is to encapsulate microorganisms whitin ceramic materials. The sol–gel method has been extensively used for the preparation of such kind of materials permitting a higher stability and viability of useful organisms. In this work, the thermal characterization during dehydration of nitrifying and denitrifying aqueous emulsions of mud encapsulated in sol–gel silica is presented during the process of dehydration in ambient conditions and as a function of temperature. The characterization was performed by a photopyroelectric (PPE) technique, whose detector was made with a 110 mm polyvinyldifluoride (PVDF). The cell was constructed in such a way that the sample was inside the cell, and the bottom of the cell was closed by the PVDF foil. Thermal effusivity as a function of temperature was obtained illuminating the PVDF directly by a modulated 1W tungsten lamp. The sample is enclosed inside a chamber, using a Peltier cell that controls temperature in a range from 40 to 27 °C. The sample is on top of the PVDF, which is illuminated by the modulated tungsten lamp.

Keywords: Nitrifying; Denitrifying; Muds; Sol–gel; Thermal properties; Photopyroelectric technique

1. Introduction

Nitrate is an important contaminant of water sources due to its high mobility and stability [1]. Several studies reveal that high concentrations of this pollutant (more than 45 mg/l) produce infant diseases as methemoglobinemia, commonly known as “infant cyanosis” and human cancer.

The problem for the elimination of nitrogenous compounds has not yet been completely solved. The physical–chemical elimination of ammoniac compounds became too expensive in waste waters with high concentration of these products. For these reasons, several research groups have focused their studies in the biological elimination of nitrogen, using microbial consortiums to reduce the nitrate concentration in waste water [2].

Biological nitrate elimination can occur by denitrifying or nitrifying processes. During denitrification, nitrate is reduced to N_2 by a wide number of heterotrophic bacteria, such as *Aerobacter*, *Klebsiella*, and *E. coli*, and few fungi, e.g., *Neurospora*. The nitrification is a process made by Gram-negative litoautotrophic unsporulated microorganisms from the family Nitrobacteriaceae.

The use of microbial muds to degrade nitrates presents some limitations, such as the contact surface area and the instability of microbial species. However, it has been proved that employing the sol–gel method to encapsulate biomolecules and microorganisms, significantly reduce restrictions [3–6]. The sol–gel process permits the encapsulations of several organic compounds and living cells due to its preparation features, such as: low temperature, high stability, pH regulation, and contact surface area. Encapsulation allows the permanent interaction between the microorganisms and the substrate, and does not harm viability and cell reproduction [3,5,7].

* Corresponding author. Tel.: +52-5-558-04-46-21; fax: +52-5-558-04-46-11.
E-mail address: mp@xanum.uam.mx (M. Picquart).

0040-6031/$ – see front matter © 2004 Elsevier B.V. All rights reserved.
doi:10.1016/j.tca.2004.04.010

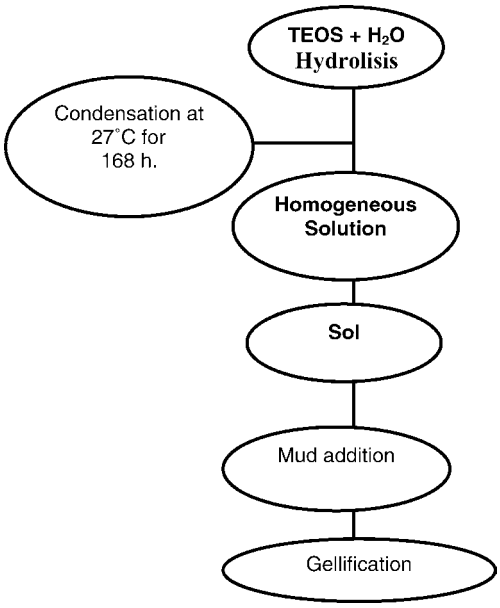

Fig. 1. Sol–gel encapsulation of microbiological muds.

2. Experimental

2.1. Mud encapsulation

Two kinds of microbial consortiums were used—denitrifying mud and nitrifying mud. Both were obtained by continuous cultures as reported by Gomez et al. [2].

The sol–gel method was employed to encapsulate the muds within a silica network, as shown in Fig. 1. Tetraethyl orthosilicate (TEOS, 99.999+%) was used as precursor and a water relationship of 1:8 was used. The mixture was kept with low stirring and ambient temperature (27 °C), 5 ml of nitrifying mud was added to the prehydrolyzed solution drop by drop until gellation. The stirring continued until gellation. The gel was aged during 168 h and then dried into a rotary evaporator system (Eseve D402-2) at ambient temperature until eliminate residues of water and alkoxide. Nitrifying mud was synthesized at pH 6, whereas denitrifying mud at pH 7.

2.2. Sample preparation

For the photoacoustic (PA) and photopyroelectric (PPE) measurements, the encapsulated muds were grinded and mixed with water in order to get a liquid suspension. The relationship, mud:water was of 1:1.5 for the denitrifying and 1:4 for the nitrifying mud.

2.3. Photoacoustic measurements

PA monitoring was carried out using the PA cell shown in Fig. 2. In this configuration the PA cell is closed at the bottom end, by a glass window and at the top end,

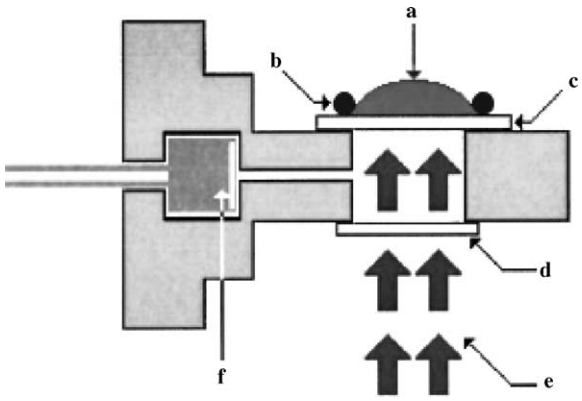

Fig. 2. Cross-section of the photoacoustic cell used: (a) sample, (b) 1 cm acrylic ring, (c) aluminum reference material, (d) quartz window, (e) modulated light, and (f) microphone.

by a removable substrate. An electret microphone is used, coupled to the cavity wall, to sense the pressure fluctuations in the PA chamber produced by the periodic heating of the substrate due to the pumping beam. This substrate is used as a reference material. The sample is deposited on the external surface of this reference material. The experimental arrangement consists of a He–Ne 25 mW laser beam, which is mechanically modulated by an optical chopper (SR540) at constant frequency ($f = 7$ Hz), for all experiments, and focused onto the reference. The microphone signal is fed into a lock-in amplifier (SR830), from where the output signal amplitude is recorded, as a function of time, in a personal computer. All measurements were performed using an aluminum foil of 50 μm thickness as the reference material, with a thermal diffusivity of 0.9 cm^2/s.

According to the Rosencwaig and Gersho model [8,9], the PA signal is determined by the temperature fluctuation, θ, at the air–substrate interface ($x = 0$). Solving the thermal diffusion equation for the configuration shown in Fig. 2, one gets

$$\theta = \theta_0 \left[\frac{b \tanh(\sigma l) + 1}{b \coth(\sigma l) + 1} \right] \quad (1)$$

here σ is the complex thermal diffusion coefficient, defined by $\sigma = (1 + i)a$, with a defined by $(\pi/f\alpha)^{1/2}$, $b = \varepsilon_b/\varepsilon$ the thermal coupling coefficient, with ε and ε_b defined as thermal effusivities of the substrate and sample, respectively. θ_0 the expression for the temperature fluctuation in the absence of the sample on the substrate, which is given by $\theta_0 = (I_0/2k)\coth(\sigma l)$. In arriving at Eq. (1), we used the fact that the effusivity of air is much smaller than the thermal effusivity of the substrate, which is optically opaque. Also, it has been considered that the optical absorption coefficient, β is much larger, that the absolute value of the complex thermal diffusion coefficient, $|\sigma|$, for the frequency is used here. Moreover, the backing thickness, l_b, is supposed to be much larger than the thermal diffusion length of the sample, which is given by

$\mu_b = (\alpha_b/\pi f)^{1/2}$, being α_b, the thermal diffusivity of the sample. From Eq. (1) the amplitude of the ratio θ/θ_0 is given by

$$q = \left|\frac{\theta}{\theta_0}\right| = \frac{\sqrt{\cosh(2al) - \cos(2al)}}{\sqrt{\cosh(2al) + \cos(2al)}} \times \frac{\sqrt{(b+1)^2 e^{2al} + (b-1)^2 e^{-2al} - 2(b^2-1)\cos(2al)}}{\sqrt{(b+1)^2 e^{2al} + (b-1)^2 e^{-2al} + 2(b^2-1)\cos(2al)}} \quad (2)$$

Solving Eq. (2) for the thermal coupling coefficient, one gets the sample effusivity

$$\varepsilon_b = \varepsilon\left(\frac{-B + \sqrt{B^2 - AC}}{A}\right) \quad (3)$$

where:

$$A = (q^2-1)\left[\cosh^2(2x) + \cos^2(2x)\right] + 2(q^2+1)\cosh(2x)\cos(2x)$$
$$B = \sinh(2x)\left[(q^2-1)\cosh(2x) + (q^2+1)\cos(2x)\right]$$
$$C = (q^2-1)\left[\cosh^2(2x) - \cos^2(2x)\right] \quad \text{and} \quad x = al$$

Measuring the evolution of $q = q(t)$, the values of $\varepsilon_b(t)$ can be obtained.

2.4. Photopyroelectric measurements

The system for determining the thermal effusivity consisted of a closed PPE cell as shown in Fig. 3. The pyroelectric film polyvinyldifluoride (PVDF) was directly illuminated by a tungsten low power lamp (2 mW) operating in modulated form using a circuit coupled to a power supply and at a given frequency fixed by the TTL output of a SR830 lock-in amplifier.

The temperature control consisted of a homemade system based on the use of a Peltier cell for temperature control coupled to a programmable power supply and a LM35DZ device for monitoring the temperature of the cell. The current provided by the power supply is regulated by a PID control system in LabView. The samples were positioned inside of the cell at 40 °C, and the measurements were performed by lowering the temperature at a rate of 1 °C/h. After each programmed change of temperature, a scan of the modulation frequency of the lamp were performed for 0.1, 0.2, 0.3, 0.4, and 0.5 Hz. The detection of the PPE signal and the control of the modulation frequency of the lamp were done, using the lock-in amplifier (SRS830), interfaced with a personal computer via a GPIB bus.

Thermal effusivity was determined directly from the experimental data, using the fact that for samples and sensor are thermally thick and thermally thin respectively; the PPE signal is inversely proportional to the effusivity of the sample [10,11]:

$$V = K\frac{\sqrt{f}}{e_m} \quad (4)$$

where K is a factor depending on the sensor, e_m the thermal effusivity of the sample, and f the modulation frequency of the lamp. The cell was calibrated, filling it with water and developing the temperature scan from 40 to 25 °C. Afterwards, the cell was filled with mud, and a scan in the same range of temperature is performed. The signal obtained for the mud is normalized using the calibration values for the water.

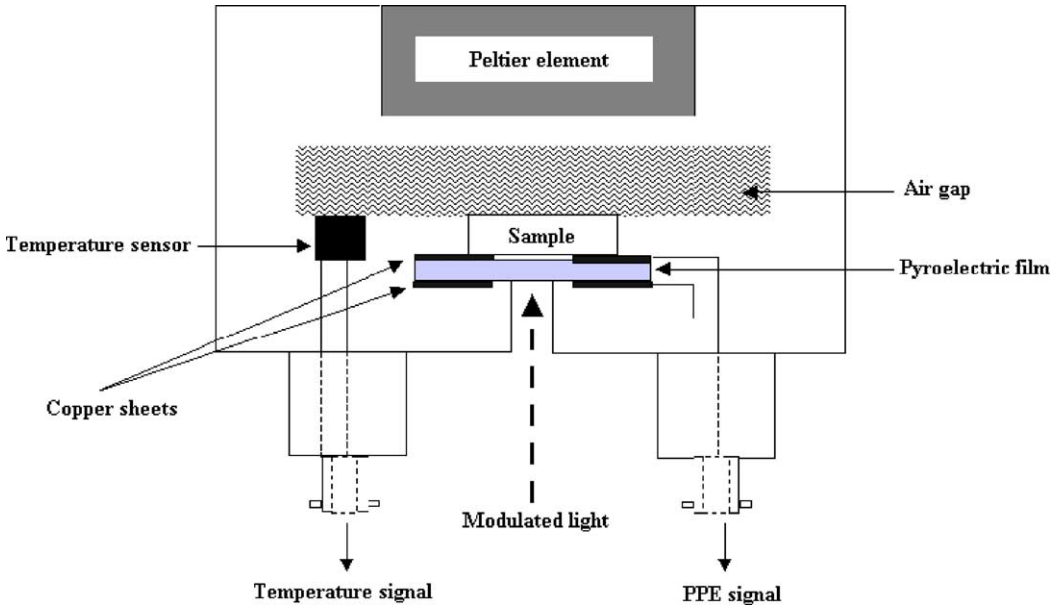

Fig. 3. Photopyroelectric cell.

3. Results

The experimental results for the PA measurements as a function of time are shown in Fig. 4. The processes begin with a low and constant signal and after some time it increases, reaching a stable level, this behavior is due to the dehydration process of the muds. The lower level corresponds to the high content of water, meanwhile the upper one is related to the dried stage. Due to the shape of the curves of the obtained data, it can assumed that a second-order kinetics is present, therefore, the data can be analyzed using a sigmoidal fitting functions of the following form:

$$S = A + \frac{B}{1 + e^{(t-t_0)/t_d}} \quad (5)$$

where S is the PA signal, t_d is related to the time interval where the maximum variation in the signal occurs and t_0 is identified as the time at which the concavity of the sigmoidal curve changes. A and B are constants related with the maxima and minima of the signals.

Using Eq. (5), the fitting values for nitrifying (Fig. 4a) and denitrifying mud (Fig. 4b), for the time when the process reaches the maximum velocity t_0, are 4.563 and 2481 s; and for the time interval in which the increasing process occurs, t_d are 110 and 277 s, respectively. Time t_0 is 1.84 larger and t_d is 0.4 times lower for nitrifying than for the denitrifying mud, as can be seen in Fig. 4a and b. These results indicate, the fact that the beginning of the dehydration process is more delayed in the nitrifying mud case. However, when the process develops, the dehydration occurs faster in the case of the nitrifying mud. Given, that the nitrifying mud presents a clay-like consistency, the results of these measurements only show the first stages of dehydration, since the whole process takes several days. Therefore, our results indicate, that in the first stages of dehydration, water is released more easily in nitrifying muds.

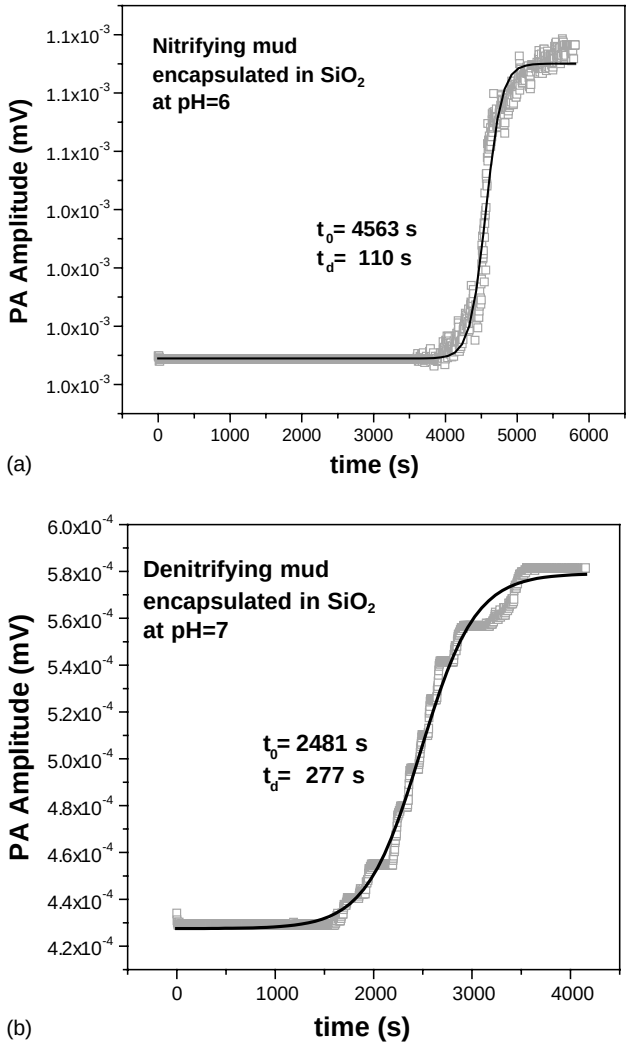

Fig. 4. Photoacoustic monitoring of the dehydration process of muds encapsulated in SiO_2 as a function of time: (a) nitrifying mud and (b) denitrifying mud.

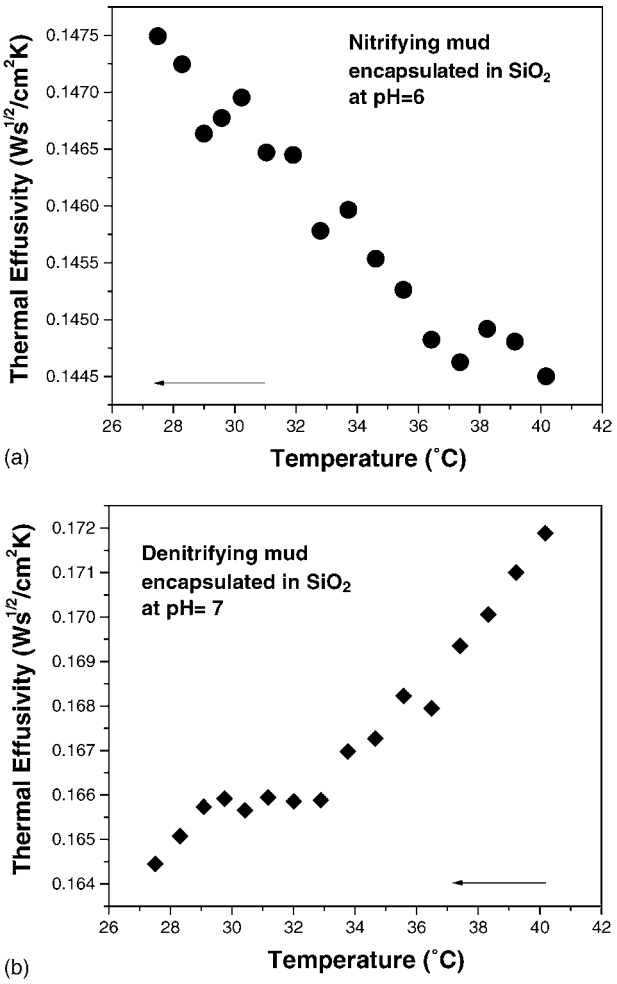

Fig. 5. Behavior of the thermal effusivity effect of microbiologicals muds when temperature diminishes: (a) nitrifying mud encapsulated in SiO_2 at pH 6 and (b) denitrifying mud encapsulated in SiO_2 at pH 7. Arrows indicate the temperature progression.

On the other hand, the measurements of the thermal effusivity, using the PPE technique, at controlled and variable temperature, presents a very different behavior for the two types of muds. In the case of nitrifying muds thermal effusivity grows when the temperature decreases (Fig. 5a), in contrast, the denitrifying mud thermal effusivity decreases for lower temperatures (Fig. 5b). This behavior can be understood, taking into account that the consistency of each mud, denitrifying ones present a gel-like aspect and dissolves easily in water. Therefore, the behavior is similar to the one found for pure water. In contrast, nitrifying mud behaves as a clay, requires more water and agitation during its preparation, showing a higher viscosity. The slight increase of thermal effusivity when the temperature is lowered can be explained by an increase in the viscosity of the mud. This increase indicates that the structure of this mud is becoming more compact and this could enhance heat diffusion. In agreement with these results, dehydration shows a delay and with a high initial velocity, indicating that free water is easily evaporated and the real process of dehydration takes much longer period of time (more than 1 day).

4. Conclusions

Dehydration process of nitrifying and denitrifying muds has been analyzed by the PA technique. The behavior of thermal effusivity, as a function of temperature has been monitored using PPE technique. Our results, show that nitrifying muds retain water for longer period of time, but release water faster in the initial stages of the dehydration process. Thermal properties are strongly influenced by the physical characteristics of the muds, denitrifying muds showing a water-like behavior, and nitrifying muds, a clay-like behavior. Our results could be very useful in the understanding of the mud with water when encapsulated in a sol–gel ceramic matrix.

Acknowledgements

The authors wish to thank J. Bante and F. Kantun for technical assistance. This work was partially supported by Conacyt Project No. 38493-U.

References

[1] J. Pacheco, L. Marin, A. Cabrera, B. Steinich, O. Escolero, Environ. Geol. 40 (2001) 708–715.
[2] J. Gomez, J. Lema, J. Mendez, Ciencia 46 (1995) 507–523.
[3] L. Zheng, K. Flora, D. Brennan, Chem. Mater. 10 (1998) 3974–3983.
[4] S. Fennouh, S. Guyon, J. Livage, C. Roux, J. Sol Gel Sci. Technol. 19 (2000) 647–649.
[5] L. Inama, S. Dire, G. Carturan, J. Biotech. 30 (1993) 197–210.
[6] R. Bhatia, C. Brinker, A. Gupta, A. Singh, Chem. Mater. 12 (2000) 2434–2441.
[7] E. Pope, K. Braun, C. Peterson, J. Sol Gel Sci. Technol. 8 (1997) 635–639.
[8] A. Rosecwaiq, Photoacoustics and Photoacoustic Spectroscopy, Wiley, New York, 1980.
[9] M. Vargas-Luna, G. Gutierrez-Juarez, J.R. Rodríguez-Vizcaino, J.B. Varela-Najera, J.M. Rodríguez-Palencia, J. Bernal-Alvarado, M. Sosa, J.J. Alvarado-Gil, J. Phys. D: Appl. Phys. 35 (2002) 1532–1537.
[10] J. Caerels, C. Glorieux, J. Thoen, Rev. Sci. Instrum. 69 (1998) 2452–2458.
[11] D. Frandas, C. Paris, M. Bissieux, J. Chirtoc, S. Antoniw, M. Egée, Appl. Phys. B 71 (2000) 69–75.